Article

J. Mex. Chem. Soc. **2022**, *66*(2)
Regular Issue

ISSN-e 2594-0317

In-silico Studies of Phytochemicals of Ashwagandha, Harsingar, Meethi neem and Tulsi Against Covid-19

Vandita Anand, Saumya Srivastava, Anjana Pandey*

Department of Biotechnology, Motilal Nehru National Institute of Technology (MNNIT), Allahabad, Prayagraj-211004, India.

***Corresponding author:** Anjana Pandey, email: anjanap@mnnit.ac.in; Tel.: +915322271233; Mobile: 09452690849.

Received August 4th, 2021; Accepted January 13th , 2022.

DOI: http://dx.doi.org/10.29356/jmcs.v66i2.1643

Abstract. The ongoing coronavirus disease 2019 (COVID-19) has become a global pandemic and risk to the healthcare system of almost every nation around the world. The endocytic pathway has been considered as a key factor in viral infection. In the case of CoVs, several investigations have shown that these viruses mainly follow the clathrin-mediated endocytic pathway. As a result, inhibiting the clathrin-mediated endocytic pathway might be a useful therapeutic approach. In this study, bioactive components of Harsingar, Meethi neem, Tulsi and Ashwagandha extract was analyzed by HR-LCMS and among them 55 phytochemical compounds were selected based on antiviral and steroidal properties. 55 phytochemical compounds of four Indian herbal plants were used to analyze their binding with clathrin protein associated with COVID -19. Based on the molecular docking as well as ADMET analysis, Ashwagandha, Harsingar, Meethi neem and Tulsi were identified as potential herbal medicine candidates. We have found that the inhibition potentials of the Ashwagandha, Harsingar, Meethi neem and Tulsi are very promising with no side effects.
Keywords: COVID-19, SARS-CoV-2, Indian herbal plants, phytochemical compounds, docking, ADMET analysis.

Resumen. La enfermedad provocada por el coronavirus 2019 (COVID-19) se ha convertido en una pandemia global y pone en riesgo a los sistemas de salud de casi cualquier nación en el mundo. Se ha considerado que la ruta endocítica es un factor clave en la infección viral. En el caso de CoVs, varias investigaciones han mostrado que estos virus siguen la ruta endocítica mediada por la clatrina. Como resultado, inhibir la ruta endocítica mediada por la clatrina puede ser una propuesta terapéutica útil. En este estudio, se analizaron extractos de componentes bioactivos de Harsingar, Meethi neem, Tulsi y Ashwagandha por HR-LCMS y entre ellos se seleccionaron 55 compuestos fitoquímicos basados en sus propiedades antivirales y esteroidales. Estos 55 compuestos obtenidos de 4 plantas herbáceas se utilizaron para analizar su interacción con la proteína clatrina asociada al COVID-19. Basados en el acoplamiento molecular, así como en el análisis ADMET, se determinó que Harsingar, Meethi neem, Tulsi y Ashwagandha son candidatos potenciales de medicinas herbáceas. Hemos encontrado que los potenciales de inhibición de Harsingar, Meethi neem, Tulsi y Ashwagandha son muy promisorios y no muestran efectos colaterales.
Palabras clave: COVID-19, SARS-CoV-2, plantas herbáceas de la India, compuestos fitoquímicos, acoplamiento molecular, análisis ADMET.

J. Mex. Chem. Soc. **2022**, *66*(2)
Regular Issue

ISSN-e 2594-0317

Introduction

Coronavirus disease (COVID-19) is a deadly disease caused by a novel severe acute respiratory syndrome coronavirus (SARS-Cov-2) that first appeared in Wuhan province in China [1, 2]. Coronaviruses (CoVs) are single-stranded positive sense RNA viruses belong to the Coronaviridae family. The genome is 26–32 kb in size and has 6–11 open reading frames (ORFs) that code for 9680 amino acid polyproteins [3]. The virus primarily affects the respiratory system, resulting in flu-like symptoms such as coughing, fever, and, in severe cases, difficulty breathing [4].

Based on genomic organization and phylogenetic relationship, coronaviruses have been classified into the subfamily Coronavirinae that consists of four genera, i.e., Alphacoronavirus (αCoV), Betacoronavirus (βCoV), Gammacoronavirus (γCoV), and Deltacoronavirus (δCoV) [5]. The surface viral protein spike, membrane, and envelope of coronavirus are embedded in the host membrane-derived lipid bilayer encapsulating the helical nucleocapsid comprising viral RNA [6]. Coronaviruses have four proteins that enclose the viral genomic RNA: membrane glycoprotein (M), nucleocapsid protein (N), envelope protein (E), and spike glycoprotein (S) [7]. After proteolytic cleavage, the S protein forms two subunits, S1 and S2, which are important in the virus entrance pathway to host cells [8]. S1 promotes receptor binding, whereas S2 helps membrane fusion; both are essential for virus entrance into the endocytic pathway. The endocytic pathway is mainly employed as the primary viral entry mechanism. It is reported that SARSCoV-2 exploits the receptor that is angiotensin converting enzyme II (ACE2) for entry into the host cells [9]. The major sites of ACE2 protein expression are epithelial cells of the human lung and small intestine [10]. Since SARS-CoV-2 also interacts with ACE2 receptor [11] and is also susceptible to inhibitors so it was assumed that it follows the same endocytic pathway for infection [12]. Entry of CoVs into the host cells is mainly mediated by the endocytic pathway, meanwhile the autophagy has also been implicated in the viral replication in the cells, a process partly related to the formation of double-membrane vesicles in the host cells. As a result, several groups of inhibitors including the lysosomotropic agents such as CQ and inhibitors for clathrin-mediated endocytosis such as chlorpromazine have been proposed to have therapeutic efficacy against CoVs-induced diseases including COVID-19 [12]. Several evidences reported that Clathrin-mediated endocytosis is the key mechanism for coronaviruses for entry into the host cell [13-15].

The paper highlights the potential antiviral activity of plant compounds as effective and reliable agents against viral infections. Various antiviral mechanisms shown by crude plant extracts and plant-derived bioactive compounds. The understanding of the action mechanisms of complex plant extract and isolated plant-derived compounds will help pave the way towards the combat of this life-threatening disease [16]. Ashwagandha (*Withania somnifera*) mentioned in Ayurveda belongs to the family Solanaceae. All parts of this plant are utilized in the prevention and cure of a wide range of ailments as it contains alkaloids, flavonoids and steroidal lactones. The root of Ashwagandha has been applied as a tonic, stimulant, astringent, aphrodisiac, anthelmintic, diuretic, thermogenic and narcotic [17]. The natural phytochemicals of Ashwagandha has distinct effects on the viral RBD (receptor-binding domain) and host ACE2 (angiotensin-converting enzyme 2) receptor complex. Natural phytochemicals may be a viable option in managing host cells for COVID-19 entry. The antiviral potential of Ashwagandha may project as potential one in fighting for management of COVID-19 infections and other virus infection because of its tremendous immuno boosting properties [18-19]. Harsingar (*Nyctanthes arbor-tristis* Linn.) belongs to the family Oleaceae. The plant has been screened for anti-malarial anti-histaminic, anti-arthritis activities, local anaesthetic, anti-hypnotic, analgesic, anti-ulcer, anti-pyretic, anti-depressant, anti-cancer, anti-larvicidal, anti-allergic, antiviral, immune modulatory, anti-helminthic, antioxidant, antidiuretic, antioxidant, and CNS modulatory properties [20-21]. Harsingar possesses antiviral activity against enveloped virus (V) [22]. *Murraya koenigii* (also known as the 'curry tree', meethi neem) is an important medicinal plant. Several parts of this plant constitute the vital ingredients of many Ayurvedic formulations such as fresh leaves, fruits, bark, and roots are used to treat several health disorders such as diabetes, bronchial disorders, vomiting and skin ailments [23]. Through various research and pharmacological evaluation, it has been shown that the plant extracts possess antiviral, anti-inflammatory, antioxidant, antidiabetic, antidiarrhoeal, antileishmanial, and antitumor activity [24]. Tulsi (*Ocimum sanctum* Linn.) belongs to the family Lamiaceae. This aromatic shrub has been reported for antidiabetic, wound healing, antioxidant, radiation protective, immunomodulatory, antifertility, anti-inflammatory, antimicrobial, antistress

J. Mex. Chem. Soc. **2022**, *66*(2)
Regular Issue

ISSN-e 2594-0317

and anti-cancer activities [25-26]. Hydro-alcoholic extract of *Ocimum sanctum* inhibited intracellular multiplication of virus. It also inhibits non-specific interference with virus-cell interactions in H9N2 viruses [27-28]. Tulsi have been revealed to target reverse transcriptase activity and have shown inhibitory actions towards HIV proteases [29].

Molecular docking plays an important role in predicting the binding modes and binding abilities of small molecules towards the targeted proteins, which is crucial in designing potential drugs [30]. In view of the above, the present investigation was undertaken to identify the active constituents of Ashwagandha, Harsingar, Meethi neem and Tulsi extracts through LC-QTOF-MS/MS analysis and an *in-silico* study was carried out to predict the molecular interaction between the clathrin and the ligands that were identified in Ashwagandha, Harsingar, Meethi neem and Tulsi extracts.

Experimental

Materials and methods

Plant material collection

Meristematic leaf of Harsingar, Meethi neem, Tulsi was collected from Motilal Nehru National Institute of Technology Allahabad, Prayagraj and dry root of Ashwagandha was collected from the shop in Teliarganj near Motilal Nehru National Institute of Technology Allahabad. The plant material was cleaned with deionized water, followed by distilled water wash, and cut into small pieces.

Preparation of Extract

About 5 g of plant material was taken and added into 100 ml of distilled water and boiled for 3 min. After boiling, the extract was filtered with Whatman filter paper and keep in the oven for drying at 50 °C for 48 hrs. After drying, the extract was dissolved in DMSO.

HR-LCMS analysis of LCME

The bioactive components of Harsingar, Meethi neem, Tulsi and Ashwagandha extract were analyzed by High Resolution Liquid Chromatograph Mass Spectrometer (HR-LCMS) G6550A system (Agilent technologies). The method used for Chromatography was 30 mins ± ESI 11012021_MSMS.m. The Gas temperature used for analysis was 250 °C and theoretical mass of protonated compound was used for identification. HR-LC-MS analysis of Harsingar, Meethi neem, Tulsi and Ashwagandha extracts was performed at Sophisticated Analytical Instrument Facility (SAIF), Indian Institute of Technology, Mumbai, India. The compounds were identified by comparison with their retention time (RT) and mass with stored metlin library available with IIT, Bombay [31]. The compounds containing a variety of bioactive constituents, such as alkaloids, phenolic compounds, saponins, flavonoids which make them a suitable treatment option against viral infections were selected [32].

Molecular Docking

Clathrin protein structure

The 3D structure of clathrin protein (PDB ID:1UTC) was downloaded from PDB (Protein Data Bank) by using URL http://www.rcsb.org/PDB in pdb format (Figure 1). The PDB structure of the clathrin protein was generated by eliminating water molecules, adding hydrogen atoms and Kollman charges. The protein file was saved in PDBQT format for future analysis, and then AutoDock Tools 1.5.6 was used to optimize the file for docking.

Ligands

Ligands were selected from the results of HR-LCMS and they were downloaded from PubChem database (https://pubchem.ncbi.nlm.nih.gov/). SMILES was used to design the structures of all compounds, and 3-D optimization was done using chemsktech software and save them in MOL format. Following that, the Open

J. Mex. Chem. Soc. **2022**, *66*(2)
Regular Issue

ISSN-e 2594-0317

Babel tool was used to convert the compounds from MOL to PDB format and save them [33]. The ligand files were saved in PDBQT format and then optimized for docking using AutoDock Tools 1.5.6 for further research.

Docking of Protein and Ligand

The molecular docking of the screened ligands with clathrin protein was performed using AutoDock 1.5.6 [34]. In this process, the grid was setup onto the clathrin protein and grid parameter file was saved. The grid map x-y-z-dimension was 47.3 Angstroms. Then target proteins were docked with screened ligands and binding energy was calculated. During the docking procedure, the various conformations for ligand were generated, but the best conformations with minimal energy were considered as output. Using the Autodock tool results were analyzed and the binding energies of all 55 ligands with clathrin protein along with H-bond formation were estimated.

ADME and Toxicity analysis

The online tool ALOGPS 2.1 (http:/www.vcclab.org/lab/alogps/) [35] was used to conduct the ADME analysis of the selected ligands and to estimate their logP and logS values. The molecular structure of compounds was submitted to ADMET-SAR server (http://lmmd.ecust.edu.cn/admetsar1/home/) [36] to analyzed their blood brain barrier penetration, carcinogenicity, subcellular localization, LD50 and category of acute oral toxicity.

Results and discussion

HR-LCMS analysis

HR-LCMS analysis of LCME resulted in the presence of phytoconstituents from Ashwagandha, Harsingar, Meethi neem and Tulsi. Among them, there are 55 compounds from Ashwagandha, Harsingar, Meethi neem and Tulsi (Table 1) were known for antiviral and steroidal properties. Medicinal plant extracts potentially improve the inherent antiviral defense mechanisms of the human body, which involve a complicated system and might use several concurrent pathways [37].

Table 1. The phytoconstituents from Ashwagandha, Harsingar, Meethi neem and Tulsi with their molecular formula.

S.No.	Compounds	Extracted from plant	Molecular Formula
1.	Ammothamnine	Ashwagandha	$C_{15}H_{24}N_2O_2$
2.	Petasinine	Ashwagandha	$C_{13}H_{21}NO_3$
3.	Fusicoccin H	Ashwagandha	$C_{26}H_{42}O_8$
4.	Stanolone benzoate	Ashwagandha	$C_{26}H_{34}O_3$
5.	16alpha,17alpha-Dihydroxyprogesterone acetophenide	Ashwagandha, Harsingar, Meethi neem, Tulsi	$C_{29}H_{36}O_4$
6.	Neohesperidin	Ashwagandha, Meethi neem	$C_{28}H_{34}O_{15}$
7.	Eugenol O-[3,4,5-Trihydroxybenzoyl-(->6)-b-D-glucopyranoside]	Ashwagandha, Meethi neem	$C_{23}H_{26}O_{11}$
8.	3beta-Hydroxy-16-phosphonopregn-5-en-20-one monoethyl ester	Ashwagandha, Harsingar, Meethi neem	$C_{23}H_{37}O_5P$
9.	Norethindrone acetate	Ashwagandha	$C_{22}H_{28}O_3$
10.	3-Hydroxycoumarin	Harsingar, Meethi neem, Tulsi	$C_9H_6O_3$
11.	Quercetin	Harsingar	$C_{15}H_{10}O_7$
12.	Kaempferol 3-rhamnoside 7-galacturonide	Harsingar	$C_{27}H_{28}O_{16}$

J. Mex. Chem. Soc. **2022**, *66*(2)
Regular Issue

ISSN-e 2594-0317

13.	Peganine	Harsingar, Meethi neem, Tulsi	$C_{11}H_{12}N_2O$
14.	Bufotalin	Harsingar	$C_{26}H_{36}O_6$
15.	Polyporusterone D	Harsingar	$C_{28}H_{44}O_5$
16.	6"-Malonylastragalin	Harsingar	$C_{24}H_{22}O_{14}$
17.	(3S,5R,6R,7E)-3,5,6-Trihydroxy-7-megastigmen-9-one	Harsingar	$C_{13}H_{22}O_4$
18.	Aromadendrin 4'-methyl ether 7-rhamnoside	Harsingar	$C_{22}H_{24}O_{10}$
19.	Geranyl acetoacetate	Harsingar	$C_{14}H_{22}O_3$
20.	7-Dehydrologanin tetraacetate	Harsingar	$C_{25}H_{32}O_{14}$
21.	Piceatannol 4'-galloylglucoside	Harsingar	$C_{27}H_{26}O_{13}$
22.	L-Menthyl acetoacetate	Harsingar	$C_{14}H_{24}O_3$
23.	Silandrin	Harsingar	$C_{25}H_{22}O_9$
24.	Maritimetin	Meethi neem, Tulsi	$C_{15}H_{10}O_6$
25.	6-C-Galactosylluteolin	Meethi neem, Tulsi	$C_{21}H_{20}O_{11}$
26.	8-Epideoxyloganin tetraacetate	Meethi neem	$C_{25}H_{34}O_{13}$
27.	Demethyloleuropein	Meethi neem	$C_{24}H_{30}O_{13}$
28.	8-Hydroxypinoresinol 8-glucoside	Meethi neem	$C_{26}H_{32}O_{12}$
29.	10-Acetoxyligustroside	Meethi neem	$C_{27}H_{34}O_{14}$
30.	trans-Caffeic acid [apiosyl-(1->6)-glucosyl] ester	Meethi neem	$C_{20}H_{26}O_{13}$
31.	Pimentol	Meethi neem	$C_{23}H_{26}O_{12}$
32.	Hesperidin	Meethi neem	$C_{28}H_{34}O_{15}$
33.	Cynaroside	Meethi neem	$C_{21}H_{20}O_{11}$
34.	Pedaliin	Meethi neem	$C_{22}H_{22}O_{12}$
35.	Tectoridin	Meethi neem	$C_{22}H_{22}O_{11}$
36.	Irisolidone 7-O-glucuronide	Meethi neem	$C_{23}H_{22}O_{12}$
37.	Solanocapsine	Tulsi	$C_{27}H_{46}N_2O_2$
38.	Apigenin 7-glucoside	Tulsi	$C_{21}H_{20}O_{10}$
39.	3-Methylellagic acid 8-rhamnoside	Tulsi	$C_{21}H_{18}O_{12}$
40.	Butin	Tulsi	$C_{15}H_{12}O_5$
41.	Fluticasone propionate	Tulsi	$C_{25}H_{31}F_3O_5S$
42.	Caffeic acid	Tulsi	C_9H_8O4
43.	Sulochrin	Tulsi	$C_{17}H_{16}O_7$
44.	Quercetin 7-glucuronide 3-rhamnoside	Tulsi	$C_{27}H_{28}O_{17}$
45.	Ginkgetin	Tulsi	$C_{32}H_{22}O_{10}$
46.	Hesperetin 3',7-O-diglucuronide	Tulsi	$C_{30}H_{34}O_{16}$
47.	Neoastilbin	Tulsi	$C_{21}H_{22}O_{11}$
48.	Sagerinic acid	Tulsi	$C_{36}H_{32}O_{16}$
49.	Chrysosplenol D	Tulsi	$C_{18}H_{16}O_8$
50.	Epicatechin-(4beta->8)-epigallocatechin 3-O-gallate	Tulsi	$C_{37}H_{30}O_{17}$
51.	Baicalin	Tulsi	$C_{21}H_{18}O_{11}$
52.	6-Methoxyaromadendrin 3-O-acetate	Tulsi	$C_{18}H_{16}O_8$
53.	Phytolaccoside E	Tulsi	$C_{42}H_{66}O_{16}$
54.	Flavonol 7-O-beta-D-glucoside	Tulsi	$C_{21}H_{20}O_9$
55.	6-Hydroxy-2-(4-hydroxyphenyl)-5,7-dimethoxy-4H-1-benzopyran-4-one	Tulsi	$C_{17}H_{14}O_6$

J. Mex. Chem. Soc. **2022**, *66*(2)
Regular Issue

ISSN-e 2594-0317

PDB Structures of selected Proteins

The retrieved PDB structure is presented in Fig. 1.

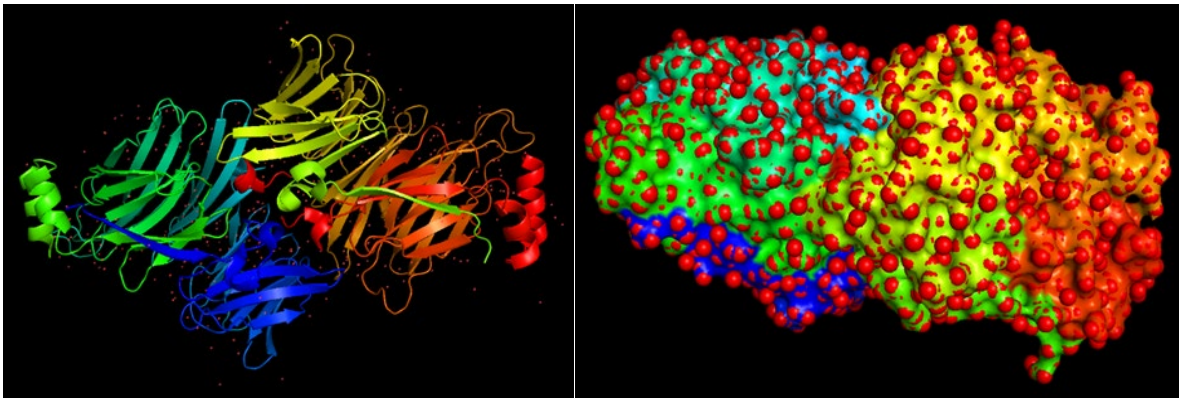

Fig. 1. 3-D structure of Clathrin protein **(a)** Ribbon view **(b)** Surface morphology.

Molecular Docking

Molecular binding studies of the clathrin protein with selected ligands were performed and estimate binding energies using AutoDock 4.2. Docking studies have been used to evaluate numerous natural or synthetic compounds as drugs against various diseases in a relatively fast and reliable manner. The lowest binding energy indicates the most significant interaction between ligand and protein [38]. Different binding positions and binding energies, as well as the bond length of H-bonds, are depicted in Table2 and Fig. 2. From the table 2 it is evident that, minimum binding energy was shown by the extracted compounds with Solanocapsine i.e., -11.34 Kcal/mol majorly followed by 16alpha,17alpha-Dihydroxyprogesterone acetophenide, Polyporusterone D, Flavonol 7-O-beta-D-glucoside, Stanolone benzoate, Ginkgetin, Norethindrone acetate, Silandrin, 6-C-Galactosylluteolin, Irisolidone 7-O-glucuronide, 3beta-Hydroxy-16-phosphonopregn-5-en-20-one monoethyl ester, Aromadendrin 4'-methyl ether 7-rhamnoside, Tectoridin, Bufotalin, Chrysosplenol D, Apigenin 7-glucoside, Butin, Baicalin, Piceatannol 4'-galloylglucoside, Hesperetin 3',7-O-diglucuronide and Cynaroside having -10.35, -9.65, -9.62, -9.61, -9.56, -9.51, -9.37, -9.25, -9.13, -9.04, -8.93, -8.83, -8.72, -8.38, -8.25, -8.24, -8.24, -8.21, -8.17 and -8.05.

The bond length of the formed H-bonds was measured thus showing the effective H-bonding between the receptor and ligand molecules. Solanocapsine formed one hydrogen bonds with LYS83 of B chain having bond lengths 2.129 Å. 16alpha,17alpha-Dihydroxyprogesterone acetophenide formed one hydrogen bonds with THR306 of chain B having bond lengths 2.09 Å. Polyporusterone D formed one hydrogen bonds with LYS83 of B chain having bond lengths 2.146 Å. Flavonol 7-O-beta-D-glucoside formed two hydrogen bonds with ASN155 and THR306 of chain A having bond lengths 2.213 and 2.025 Å respectively. Stanolone benzoate formed one hydrogen bonds with MET32 of B chain having bond lengths 2.125 Å. Ginkgetin formed one hydrogen bonds ALA172 of A chain having bond lengths 2.191 Å. Norethindrone acetate formed one hydrogen bonds with LYS83 of B chain having bond lengths 1.766 Å. Silandrin formed three hydrogen bonds with TRP111, ASN155 and GLN265 of chain B having bond lengths 1.839, 1.814 and 1.816 Å respectively. 6-C-Galactosylluteolin formed two hydrogen bonds with MET32 and TRP111 of B chain having bond lengths 1.823 and 2.056 Å respectively. Irisolidone 7-O-glucuronide formed three hydrogen bonds with LYS43 of A chain, LYS278 of B chain and ARG320 of chain B having bond lengths 1.888, 1.97 and 2.114 Å respectively. 3beta-Hydroxy-16-phosphonopregn-5-en-20-one monoethyl ester formed three hydrogen bonds LYS43 of A chain, LYS278 of B chain and ARG320 of B chain having bond lengths 2.157, 1.749 and 2.162 Å respectively. Aromadendrin 4'-methyl ether 7-rhamnoside formed two hydrogen bonds ASP124 of A chain and ARG144 of B chain having bond lengths 1.974 and 1.721 Å respectively. Tectoridin formed two hydrogen bonds with TRP111 and THR306 of chain A having bond lengths 2.117 and 2.154 Å respectively. Bufotalin formed three

J. Mex. Chem. Soc. **2022**, *66*(2)
Regular Issue

ISSN-e 2594-0317

hydrogen bonds with GLN152 of A chain, LYS278 of A chain and LYS43 of chain B having bond lengths 1.982, 2.175 and 2.032 Å respectively. Chrysosplenol D formed one hydrogen bonds THR306 of A chain having bond lengths 2.134 Å. Apigenin 7-glucoside formed two hydrogen bonds with ARG144 and ILE153 of chain B having bond lengths 1.695 and 2.1 Å respectively. Butin formed three hydrogen bonds with ARG172, SER70 and TRP111 of B chain having bond lengths 1.823, 2.045 and 1.82 Å respectively. Baicalin formed five hydrogen bonds with LYS43 of A chain, LYS43 of A chain, LYS278 of B chain, THR306 of B chain and ARG320 of chain B having bond lengths 1.789, 2.03, 1.881, 1.978 and 1.609 Å respectively. Piceatannol 4'-galloylglucoside formed three hydrogen bonds with TRP111, GLN152 and ILE153 of chain A having bond lengths 1.843, 2.134 and 1.882 Å respectively. Hesperetin 3',7-O-diglucuronide formed three hydrogen bonds with ARG41, ARG41 and LYS43 of B chain having bond lengths 2.126, 2.119 and 2.056 Å respectively. Cynaroside formed one hydrogen bonds THR306 of A chain having bond lengths 2.216 Å. Rest of the ligands having higher binding energy show lower binding affinity with clathrin protein.

Table 2. Docking results of selected ligands with clathrin protein.

S.No.	Compound name	Binding Energy (kcal/mol)	Bond length (Å)	Chain	Residue
1.	Ammothamnine	-7.38	2.098	A	LYS112
2.	Petasinine	-6.27	1.753	A	THR306
3.	Fusicoccin H	-5.69	1.971	A	ALA48
4.	Stanolone benzoate	-9.61	2.125	B	MET32
5.	16alpha,17alpha-Dihydroxyprogesterone acetophenide	-10.35	2.09	B	THR306
6.	Neohesperidin	-7.04	2.179	B	LYS83
7.	Eugenol O-[3,4,5-Trihydroxybenzoyl-(->6)-b-D-glucopyranoside]	-7.11	2.139	A	ASN155
8.	3beta-Hydroxy-16-phosphonopregn-5-en-20-one monoethyl ester	-9.04	2.157 1.749 2.162	A B B	LYS43 LYS278 ARG320
9.	Norethindrone acetate	-9.51	1.766	B	LYS83
10.	3-Hydroxycoumarin	-6.5	2.011 1.756 1.823	B	MET264 ALA199 ARG157
11.	Quercetin	-7.63	1.937	B	THR306
12.	Kaempferol 3-rhamnoside 7-galacturonide	-6.87	2.179 1.993 1.852 1.753 2.095	A B A A A	ARG41 LYS278 TRP111 LYS43 ILE153
13.	Peganine	-6.32	1.889	B	THR306
14.	Bufotalin	-8.72	1.982 2.175 2.032	A A B	GLN152 LYS278 LYS43
15.	Polyporusterone D	-9.65	2.146	B	LYS83
16.	6"-Malonylastragalin	-7.92	1.797	B	SER67
17.	(3S,5R,6R,7E)-3,5,6-Trihydroxy-7-megastigmen-9-one	-6.72	2.138 1.955	A	TRP111 LYS83

J. Mex. Chem. Soc. **2022**, *66*(2)
Regular Issue

ISSN-e 2594-0317

18.	Aromadendrin 4'-methyl ether 7-rhamnoside	-8.93	1.974 1.721	A B	ASP124 ARG144
19.	Geranyl acetoacetate	-6.18	2.238 2.219	A	ASN155 GLN265
20.	7-Dehydrologanin tetraacetate	-6.99	2.195 2.071 1.921 1.99	A B B B	ARG41 PHE27 ARG320 ARG320
21.	Piceatannol 4'-galloylglucoside	-8.21	1.843 2.134 1.882	A	TRP111 GLN152 ILE153
22.	L-Menthyl acetoacetate	-6.86	1.764	B	ALA71
23.	Silandrin	-9.37	1.839 1.814 1.816	B	TRP111 ASN155 GLN265
24.	Maritimetin	-7.53	2.058	A	TRP111
25.	6-C-Galactosylluteolin	-9.25	1.823 2.056	B	MET32 TRP111
26.	8-Epideoxyloganin tetraacetate	-6.86	1.865 1.98 2.039	A A B	ARG144 ILE153 LYS83
27.	Demethyloleuropein	-4.59	1.656 2.057 1.981 2.108 1.734	A B B B B	LYS278 ARG41 LYS43 LYS43 ALA48
28.	8-Hydroxypinoresinol 8-glucoside	-6.76	1.987	B	ARG320
29.	10-Acetoxyligustroside	-6.31	1.58	A	ILE153
30.	trans-Caffeic acid [apiosyl-(1->6)-glucosyl] ester	-5.98	2.065 2.073 2.048 2.003	B	LYS278 THR302 THR306 ARG320
31.	Pimentol	-6.21	2.232	B	ILE153
32.	Hesperidin	-7.57	1.721 1.838	A	LYS83 ILE153
33.	Cynaroside	-8.05	2.216	A	THR306
34.	Pedaliin	-7.57	2.125	A	TRP111
35.	Tectoridin	-8.83	2.117 2.154	A	TRP111 THR306
36.	Irisolidone 7-O-glucuronide	-9.13	1.888 1.97 2.114	A B B	LYS43 LYS278 ARG320
37.	Solanocapsine	-11.34	2.129	B	LYS83
38.	Apigenin 7-glucoside	-8.25	1.695 2.1	B	ARG144 ILE153
39.	3-Methylellagic acid 8-rhamnoside	-7.03	1.879 2.038 2.084	A B B	ALA172 SER70 TRP111

J. Mex. Chem. Soc. **2022**, *66*(2)
Regular Issue

ISSN-e 2594-0317

40.	Butin	-8.24	1.823 2.045 1.82	B	ARG157 MET264 THR306
41.	Fluticasone propionate	-7.78	2.046	B	THR306
42.	Caffeic acid	-7.05	1.839 1.828 1.997	A A B	ARG41 LYS43 LYS278
43.	Sulochrin	-6.12	1.732 1.756	A	SER70 LYS83
44.	Quercetin 7-glucuronide 3-rhamnoside	-6.42	2.117 2.056 1.992 1.646 1.718 1.931	A A A B B B	GLN152 GLN152 ALA172 ARG144 GLY150 GLN152
45.	Ginkgetin	-9.56	2.191	A	ALA172
46.	Hesperetin 3',7-O-diglucuronide	-8.17	2.126 2.119 2.056	B	ARG41 ARG41 LYS43
47.	Neoastilbin	-7.83	1.961 2.151	B	ALA199 THR306
48.	Sagerinic acid	-5.64	2.165 1.988 1.702 1.998	B	SER70 TRP111 ARG144 ILE153
49.	Chrysosplenol D	-8.38	2.134	A	THR306
50.	Epicatechin-(4beta->8)-epigallocatechin 3-O-gallate	-7.89	2.004 1.8	A	ARG144 GLY150
51.	Baicalin	-8.24	1.789 2.03 1.881 1.978 1.609	A A B B B	LYS43 LYS43 LYS278 THR306 ARG320
52.	6-Methoxyaromadendrin 3-O-acetate	-7.6	2.085 2.197	B	GLN265 THR306
53.	Phytolaccoside E	-7.88	2.091 2.194 1.932	A	ARG41 LYS83 ILE153
54.	Flavonol 7-O-beta-D-glucoside	-9.62	2.213 2.025	A	ASN155 THR306
55.	6-Hydroxy-2-(4-hydroxyphenyl)-5,7-dimethoxy-4H-1-benzopyran-4-one	-7.66	2.081	B	THR306

J. Mex. Chem. Soc. **2022**, *66*(2)
Regular Issue

ISSN-e 2594-0317

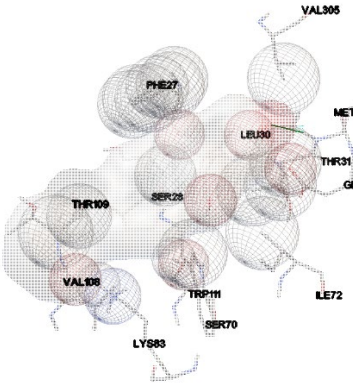

Stanolone benzoate

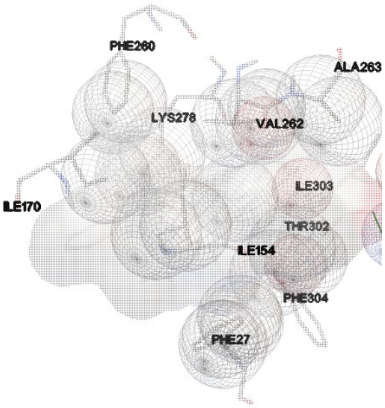

16alpha,17alpha-Dihydroxyprogesterone acetophenide

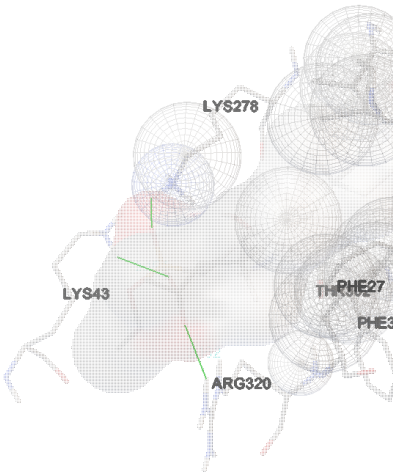

3beta-Hydroxy-16-phosphonopregn-5-en-20-one monoethyl ester

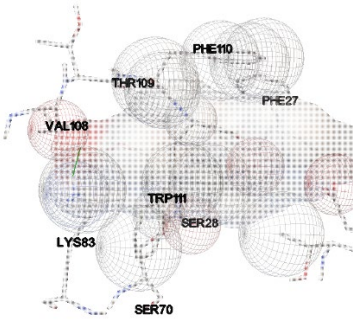

Norethindrone acetate

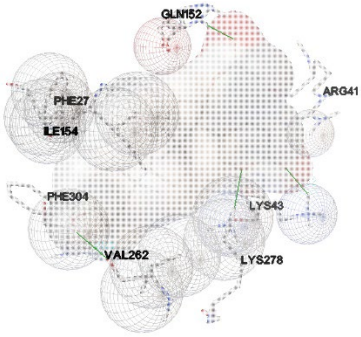

Bufotalin

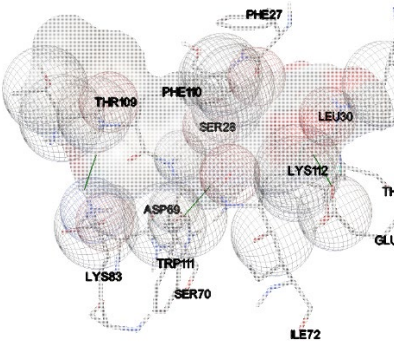

Polyporusterone D

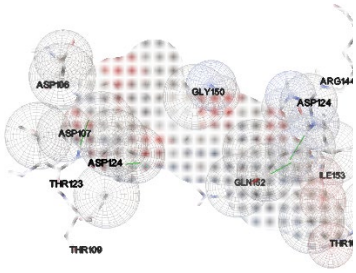

Aromadendrin 4'-methyl ether 7-rhamnoside

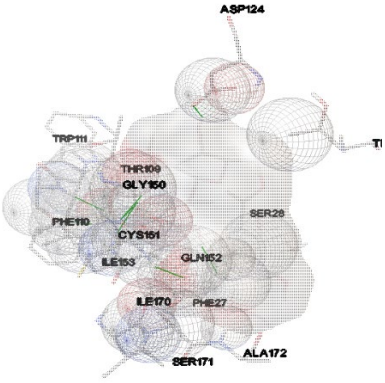

Piceatannol 4'-galloylglucoside

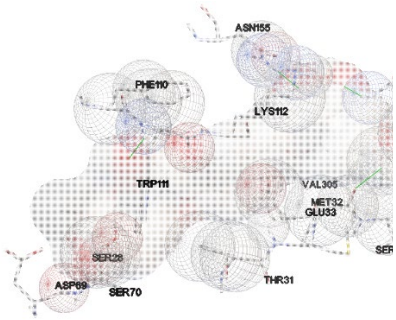

Silandrin

J. Mex. Chem. Soc. **2022**, *66*(2)
Regular Issue

ISSN-e 2594-0317

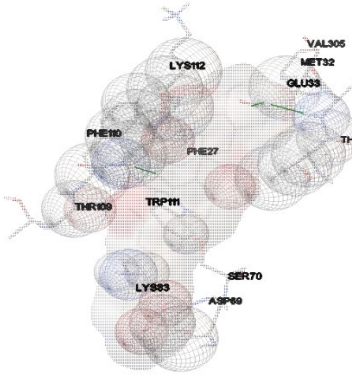

6-C-Galactosylluteolin

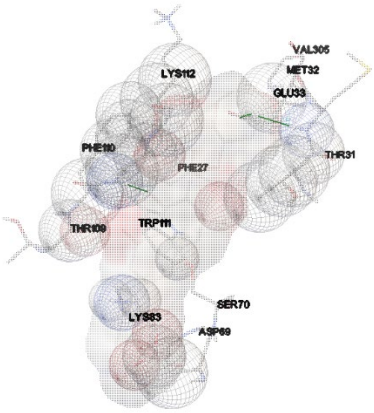

Cynaroside

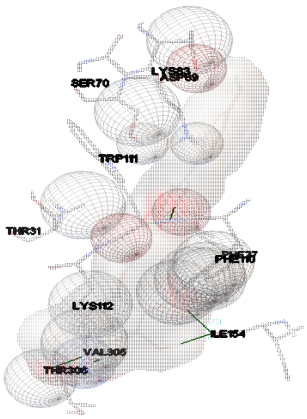

Tectoridin

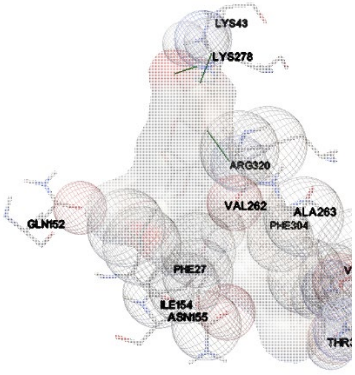

Irisolidone 7-O-glucuronide

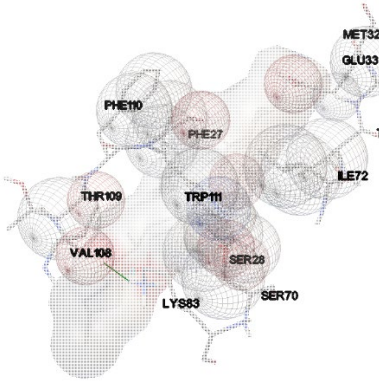

Solanocapsine

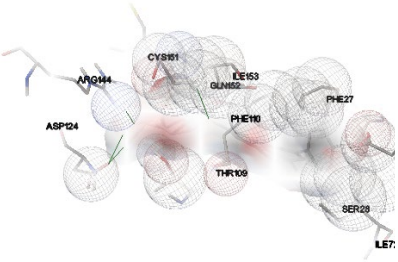

Apigenin 7-glucoside

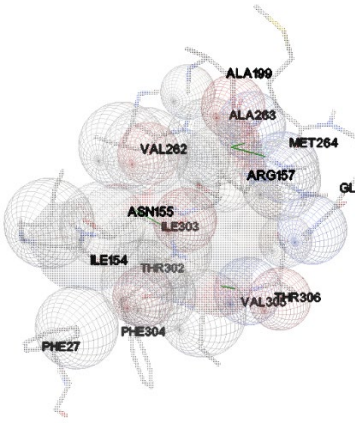

Butin

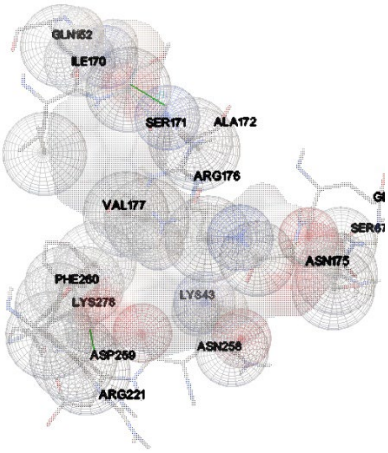

Ginkgetin

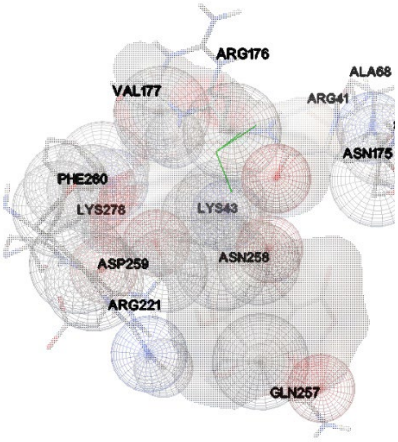

Hesperetin 3',7-O-diglucuronide

J. Mex. Chem. Soc. **2022**, *66*(2)
Regular Issue

ISSN-e 2594-0317

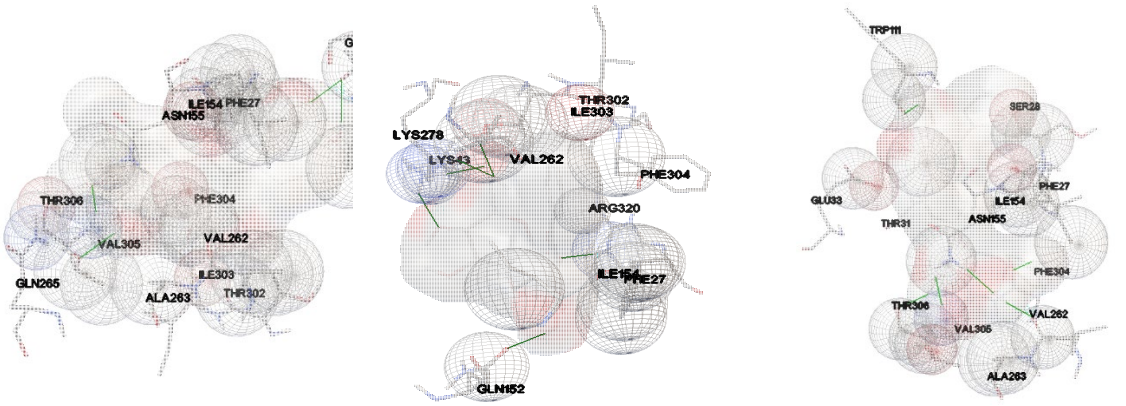

Chrysosplenol D Baicalin Flavonol 7-O-beta-D-glucoside

Fig. 2. Docking poses of selected ligands with Clathrin protein.

ADME and Toxicity analysis

The ADME analysis was done via ALOGPS tool and the logP represents lipophilicity of drug defining the drug partition in water and octane at equilibrium. Hence this parameter provides the significance of the drug into the cells. According to Lipinski's rule, the safe and permissible range of logP value is between 0-5 [39]. These values indicate that the compounds can quickly diffuse across the cell membranes due to their high organic (lipid) permeability. It is evident from Table 3 that, except Ammothamnine, Neohesperidin, trans-Caffeic acid [apiosyl-(1->6)-glucosyl] ester and Hesperidin, all other ligands exhibit positive logP values. However, all the compounds except 16alpha,17alpha-Dihydroxyprogesterone acetophenide exhibited logP values lower than 5.

LogS measures the aqueous solubility, which is significant physical property related to ADME profile of a compound. The logS values of most of these compounds are more than -5 [40], except Stanolone benzoate, 16alpha,17alpha-Dihydroxyprogesterone acetophenide, Solanocapsine and Ginkgetin (Table 3).

The toxicity of the selected phytocompounds was predicted using admetSAR. The parameters including blood-brain barrier (BBB) penetration, subcellular localization, LD50 and rat acute oral toxicity were estimated and are represented in Table 3 [36]. From the results, it is evident that none of the compounds exhibited carcinogenicity.

Compounds are classified into four categories based on their acute oral toxicity (ADMET prediction profile). The majority of the ligands showed acute oral toxicity category III, indicating that their LD50 values are in the range of 500 mg/kg to 5000 mg/kg body weight. Bufotalin was shown to have a category I acute oral toxicity, indicating that its LD50 values were less than or equal to 50 mg/kg. 3-Hydroxycoumarin, Quercetin, Maritimetin, Butin, Sulochrin, Chrysosplenol D, and Baicalin are among the compounds in Category II, having LD50 values more than 50 mg/kg but less than 500 mg/kg. 6-C-Galactosylluteolin, Caffeic acid and Epicatechin-(4beta->8)-epigallocatechin 3-O-gallate have LD50 values more than 5000 mg/kg were classified as Category IV.

On the basis of Molecular docking, the potential compound suggested was Solanocapsine, 16alpha,17alpha-Dihydroxyprogesterone acetophenide, Polyporusterone D, Flavonol 7-O-beta-D-glucoside, Stanolone benzoate, Ginkgetin, Norethindrone acetate, Silandrin, 6-C-Galactosylluteolin, Irisolidone 7-O-glucuronide, 3beta-Hydroxy-16-phosphonopregn-5-en-20-one monoethyl ester. On the basis of ADME analysis, the compound suggested was Solanocapsine, Polyporusterone D, Flavonol 7-O-beta-D-glucoside, Stanolone benzoate, Ginkgetin, Norethindrone acetate, Silandrin, 6-C-Galactosylluteolin, Irisolidone 7-O-glucuronide, 3beta-Hydroxy-16-phosphonopregn-5-en-20-one monoethyl ester. The toxicity results suggested that Solanocapsine is the most potential candidate predicted to be found in the Lysosome according to Table 3 and as well as the strongest binding affinity to Clathrin protein.

J. Mex. Chem. Soc. **2022**, *66*(2)
Regular Issue

ISSN-e 2594-0317

Table 3. ADME and Toxicity analysis of selected phytocompounds.

		ADME		TOXICITY				
S.NO.	**Extracted compounds**	**LogP**	**LogS**	**Subcellular localization**	**Carcinogenicity**	**Acute Oral Toxicity**	**BBB**	**LD50**
1.	Ammothamnine	-0.33	-2.24	Mitochondria	No	III	+	2.5699
2.	Petasinine	1.12	-0.60	Mitochondria	No	III	+	2.5538
3.	Fusicoccin H	0.86	-2.80	Mitochondria	No	III	+	3.1485
4.	Stanolone benzoate	4.91	-6.38	Mitochondria	No	III	+	1.7166
5.	16alpha,17alpha-Dihydroxyprogesterone acetophenide	5.20	-6.10	Mitochondria	No	III	+	2.9411
6.	Neohesperidin	-0.27	-2.26	Mitochondria	No	III	-	2.4045
7.	Eugenol O-[3,4,5-Trihydroxybenzoyl-(->6)-b-D-glucopyranoside]	1.79	-2.84	Mitochondria	No	III	-	2.6006
8.	3beta-Hydroxy-16-phosphonopregn-5-en-20-one monoethyl ester	2.95	-4.32	Mitochondria	No	III	+	2.4148
9.	Norethindrone acetate	3.58	-4.80	Mitochondria	No	III	+	1.8958
10.	3-Hydroxycoumarin	1.09	-1.86	Mitochondria	No	II	+	2.5276
11.	Quercetin	1.81	-3.06	Mitochondria	No	II	-	3.0200
12.	Kaempferol 3-rhamnoside 7-galacturonide	0.36	-2.30	Mitochondria	No	III	-	2.5907
13.	Peganine	0.74	-1.79	Mitochondria	No	III	+	2.7329
14.	Bufotalin	2.84	-4.52	Mitochondria	No	I	+	4.4313
15.	Polyporusterone D	2.78	-3.73	Mitochondria	No	III	+	2.9867
16.	6''-Malonylastragalin	1.21	-2.81	Mitochondria	No	III	-	2.7823
17.	(3S,5R,6R,7E)-3,5,6-Trihydroxy-	0.58	-1.57	Mitochondria	No	III	+	2.6300

J. Mex. Chem. Soc. **2022**, *66*(2)
Regular Issue

ISSN-e 2594-0317

	7-megastigmen-9-one							
18.	Aromadendrin 4'-methyl ether 7-rhamnoside	0.63	-2.41	Mitochondria	No	III	-	2.6861
19.	Geranyl acetoacetate	3.70	-3.34	Mitochondria	No	III	+	1.4700
20.	7-Dehydrologanin tetraacetate	1.01	-2.66	Mitochondria	No	III	+	3.1883
21.	Piceatannol 4'-galloylglucoside	2.11	-3.34	Mitochondria	No	III	+	2.6315
22.	L-Menthyl acetoacetate	3.18	-3.79	Mitochondria	No	III	+	1.7131
23.	Silandrin	3.08	-4.44	Mitochondria	No	III	-	2.5289
24.	Maritimetin	2.70	-3.34	Mitochondria	No	II	+	2.4653
25.	6-C-Galactosylluteolin	0.39	-2.34	Mitochondria	No	IV	-	2.3664
26.	8-Epideoxyloganin tetraacetate	1.98	-3.08	Mitochondria	No	III	+	2.9306
27.	Demethyloleuropein	0.53	-2.70	Mitochondria	No	III	-	2.3730
28.	8-Hydroxypinoresinol 8-glucoside	0.61	-2.74	Mitochondria	No	III	-	3.1133
29.	10-Acetoxyligustroside	0.51	-2.96	Mitochondria	No	III	-	2.7323
30.	trans-Caffeic acid [apiosyl-(1->6)-glucosyl] ester	-1.18	-1.88	Mitochondria	No	III	+	2.4940
31.	Pimentol	1.61	-2.70	Mitochondria	No	III	-	2.6006
32.	Hesperidin	-0.27	-2.36	Mitochondria	No	III	-	2.6228
33.	Cynaroside	0.58	-2.62	Mitochondria	No	III	-	2.3869
34.	Pedaliin	0.66	-2.66	Mitochondria	No	III	-	2.2498
35.	Tectoridin	0.62	-2.71	Mitochondria	No	III	-	2.2498
36.	Irisolidone 7-O-glucuronide	1.18	-2.73	Mitochondria	No	III	-	2.7471
37.	Solanocapsine	3.63	-6.10	Lysosome	No	III	+	2.6209
38.	Apigenin 7-glucoside	0.68	-2.65	Mitochondria	No	III	-	2.3755

J. Mex. Chem. Soc. **2022**, *66*(2)
Regular Issue

ISSN-e 2594-0317

39.	3-Methylellagic acid 8-rhamnoside	1.05	-2.28	Mitochondria	No	III	-	2.6315
40.	Butin	2.55	-3.16	Mitochondria	No	II	-	3.0230
41.	Fluticasone propionate	3.69	-4.64	Mitochondria	No	III	+	2.3753
42.	Caffeic acid	1.67	-2.05	Mitochondria	No	IV	-	1.4041
43.	Sulochrin	2.51	-3.72	Mitochondria	No	II	+	2.9889
44.	Quercetin 7-glucuronide 3-rhamnoside	0.50	-2.15	Mitochondria	No	III	-	2.5907
45.	Ginkgetin	4.96	-5.30	Mitochondria	No	III	-	2.8985
46.	Hesperetin 3',7-O-diglucuronide	0.06	-2.33	Mitochondria	No	III	-	3.0497
47.	Neoastilbin	0.79	-2.09	Mitochondria	No	III	-	2.5458
48.	Sagerinic acid	3.91	-3.79	Mitochondria	No	III	-	2.6462
49.	Chrysosplenol D	2.88	-3.70	Mitochondria	No	II	-	2.9468
50.	Epicatechin-(4beta->8)-epigallocatechin 3-O-gallate	3.20	-3.83	Mitochondria	No	IV	-	2.4797
51.	Baicalin	1.27	-2.41	Mitochondria	No	II	-	2.7357
52.	6-Methoxyaromadendrin 3-O-acetate	2.62	-3.28	Mitochondria	No	III	-	3.1632
53.	Phytolaccoside E	1.38	-3.37	Mitochondria	No	III	-	3.4672
54.	Flavonol 7-O-beta-D-glucoside	0.68	-2.61	Mitochondria	No	III	-	2.3869
55.	6-Hydroxy-2-(4 hydroxyphenyl)-5,7 dimethoxy-4H-1-benzopyran-4-one	3.22	-3.88	Mitochondria	No	III	-	3.0584

Conclusion

SARS-CoV-2 and COVID-19 have emerged as a health threat worldwide in a recent situation. The evidence from different studies have already shown that clathrin mediated endocytic pathway is a key factor in mediating viral infection. In this study, we have tried to search and identify the drugs for preventing the corona virus infection via *in silico* method. Ashwagandha, Harsingar, Meethi neem and Tulsi is an important medicinal

J. Mex. Chem. Soc. **2022**, *66*(2)
Regular Issue

ISSN-e 2594-0317

plant widely used in traditional medicine. The findings of this research study demonstrate that the leaves of Harsingar, Meethi neem and Tulsi and root of Ashwagandha possess a strong antiviral capacity. LC-MS-QTOF analysis, as well as molecular docking studies, led to the tentative identification of the compounds that are likely to be responsible for the antiviral effect of these plant. After the screening Solanocapsine is the only compound predicted to have one of the strongest binding affinity with Clathrin protein and the ADMET results exhibit their drugability. Further research is needed to obtain such bioactive compounds in pure form for complete pharmacological evaluations.

Acknowledgments

Authors are thankful to Director of MNNIT & Department of Biotechnology MNNIT Allahabad, Prayagraj, India.

References

1. Huang, C.; Wang, Y.; Li, X.; Ren, L.; Zhao, J.; Hu, Y.; Zhang, L.; Fan, G.; Xu, J.; Gu, X. *The Lancet.* **2020**, *395*, 497-506. DOI: 10.1016/S0140-6736(20)30183-5
2. Li, Q.; Guan, X.; Wu, P.; Wang, X.; Zhou, L.; Tong, Y.; Ren, R.; Leung, K. S.; Lau, E. H.; Wong, J. Y. *N. Engl. J. Med. 2020*. DOI: 10.1056/NEJMoa2001316
3. Guo, Y. R.; Cao, Q. D.; Hong, Z. S.; Tan, Y. Y.; Chen, S. D.; Jin, H. J.; Tan, K. S.; Wang, D. Y.; Yan, Y. *Mil. Med. Res.* **2020**, *7*, 11. DOI: 10.1186/s40779-020-00240-0
4. Zou, L.; Ruan, F.; Huang, M.; Liang, L.; Huang, H.; Hong, Z.; Yu, J.; Kang, M.; Song, Y.; Xia, J. *N. Engl. J. Med.* **2020**, *382*, 1177-1179. DOI: 10.1056/NEJMc2001737
5. Cui, J.; Li, F.; Shi, Z. L. *Nat. Rev. Microbiol.* **2019**, *17*, 181–192. DOI: 10.1038/s41579-018-0118-9
6. Finlay, B. B.; See, R. H.; Brunham, R. C. *Nat. Rev. Microbiol.* **2004**, *2*, 602–607. DOI: 10.1038/nrmicro930
7. de Haan, C. A.; Rottier, P. *J. Adv. Virus Res.* **2005**, *64*, 165-230. DOI: 10.1016/S0065-3527(05)64006-7
8. Millet, J. K.; Whittaker, G. R. *Virology.* **2018**, 517, 3-8. DOI: 10.1016/j.virol.2017.12.015
9. Kuba, K.; Imai, Y.; Rao, S.; Gao, H.; Guo, F.; Guan, B.; Huan, Y.; Yang, P.; Zhang, Y.; Deng, W.; Bao, L. *Nat. Med.* **2005**, *11*, 875-879. DOI: 10.1038/nm1267
10. Hamming, I.; Timens, W.; Bulthuis, M. L. C.; Lely, A. T.; Navis, G. V.; van Goor, H. *J. Pathol.* **2004**, *203*, 631-637. DOI: 10.1002/path.1570
11. Zumla, A.; Chan, J. F.; Azhar, E. I.; Hui, D. S.; Yuen, K. Y. *Nat. Rev. Drug Discovery.* **2016**, *15*, 327-347. DOI: 10.1038/nrd.2015.37
12. Yang, N.; Shen, H. M. *Int. J. Biol. Sci.* **2020**, *16*, 1724. DOI: 10.7150/ijbs.45498
13. Stadler, K.; Ha, H. R.; Ciminale, V.; Spirli, C.; Saletti, G.; Schiavon, M.; Bruttomesso, D.; Bigler, L.; Follath, F.; Pettenazzo, A.; Baritussio, A. *Am. J. Respir. Cell Mol. Biol.* **2008**, *39*, 142-149. DOI: 10.1016/j.bbadis.2020.165889
14. Pu, Y.; Zhang, X. *J. Virol.* **2008**, *82*, 8112-8123. DOI: 10.1128/JVI.00837-08
15. Burkard, C.; Verheije, M. H.; Wicht, O.; van Kasteren, S. I.; van Kuppeveld, F. J.; Haagmans, B. L.; Pelkmans, L.; Rottier, P. J.; Bosch, B. J.; de Haan, C. A. *PLoS Pathog.* **2014**, *10*, 1004502. DOI: 10.1371/journal.ppat.1004502

J. Mex. Chem. Soc. **2022**, *66*(2)
Regular Issue

ISSN-e 2594-0317

16. Abiri, R.; Abdul-Hamid, H.; Sytar, O.; Abiri, R.; Bezerra de Almeida, E., Jr.; Sharma, S. K.; Bulgakov, V. P.; Arroo, R. R. J.; Malik, S. *Molecules.* **2021**, *26*, 3868. DOI: 10.3390/molecules26133868
17. Singh, R.; Sharma, R. R.; Kumar, S.; Gupta, R. K.; Patil, R. T. *Bioresour. Tech.* **2008**, *99*, 8507-8511. DOI: 10.1016/j.biortech.2008.03.034
18. Kumar, N.; Shala, A. Y.; Khurana, S. M. P. Int. J. *Phytomed. Related Industries.* **2021**, *13*, 229-236. DOI: 10.5958/0975-6892.2021.00026.5
19. Chikhale, R. V.; Gurav, S. S.; Patil, R. B.; Sinha, S. K.; Prasad, S. K.; Shakya, A.; Shrivastava, S. K.; Gurav, N. S.; Prasad, R. S. *J. Biomol. Struct. Dyn.* **2020**, *39*, 4510-4521. DOI: 10.1080/07391102.2020.1778539
20. Desai, S. V.; Dhumal, A. S.; Chauhan, P. S. *Int. J. Pharm. Technol.* **2016**, *8*, 3611–3628.
21. Parekh, S.; Soni, A. *J. Appl. Biol. Biotechnol.* **2020**, *8*, 95-104. DOI: 10.7324/JABB.2020.80116
22. Gupta, P.; Bajpai, S. K.; Chandra, K.; Singh, K. L.; Tandon, J. S. *Indian J. Exp. Biol.* **2005**, *43*, 1156–60.
23. Samanta, S. K.; Kandimalla, R.; Gogoi, B.; Dutta, K. N.; Choudhury, P.; Deb, P. K.; Devi, R.; Pal, B. C.; Talukdar, N. C. *Pharmacol. Res.* **2017**. DOI: 10.1016/j.phrs.2017.11.024
24. Gupta, P.; Nahata, A.; Dixit, V. K. *J. Chin. Integr. Med.* **2011**, *9*, 824-833. DOI: 10.4236/ajps.2014.519302
25. Gholap, S.; Kar, A. *Pharmazie.* **2004**, *59*, 876–878. DOI:
26. Udupa, S. L.; Shetty, S.; Udupa, A. L.; Somayaji, S. N. *Indian J. Exp. Biol.* **2006**, *44*, 49–54.
27. Ghoke, S. S.; Sood, R.; Kumar, N.; Pateriya, A. K.; Bhatia, S.; Mishra, A. *BMC Complementary Altern. Med.* **2018**, *18*, 174. DOI: 10.1186/s12906-018-2238-1
28. Ahmad, S.; Zahiruddin, S.; Parveen, B.; Basist, P.; Parveen, A.; Gaurav; Parveen, R.; Ahmad, M. *Front. Pharmacol.* **2021**, *11*, 578970. DOI: 10.3389/fphar.2020.578970
29. Rege, A.; Chowdhary, A. S. *Int. J. Pharm. Sci. Rev. Res.* **2014**, *25*, 315–318.
30. Hombalimath, V. S.; Shet, A. R. *J. Adv. Bioinforma. Appl. Res.* **2012**, *3*, 345–356.
31. Shivakumar, R.; Venkatarangaiah, K.; Shastri, S.; Naga¬raja, R. B.; Sheshagiri, A. *Pharmacog. J.* **2018**, *10*, 1221-1229. DOI: 10.5530/pj.2018.6.209
32. Ghildiyal, R.; Prakash, V.; Gabrani, R. Springer Nature 2020, 279-295. DOI: 10.1007/978-981-15-1761-7_12
33. Singha, I.; Saxena, S.; Gautam, S.; Saha, A.; Das, S. K. *Indian J. Biochem. Biophys.* **2020**, *57*, 219.
34. Ganeshpurkar, A.; Saluja, A. *Indian J. Biochem. Biophys.* **2018**, *55*, 88. DOI: http://nopr.niscair.res.in/handle/123456789/44348
35. Tetko, I. V.; Tanchuk, V. Y. *J. Chem. Inf. Comput. Sci.* **2002**, *42*, 1136. DOI: 10.1021/ci025515j
36. Cheng, F.; Li, W.; Zhou, Y.; Shen, J.; Wu, Z.; Liu, G.; Lee, P. W.; Tang, Y. *J. Chem. Inf. Model.* **2012**, *52*, 3099. DOI: 10.1021/ci300367a
37. Webster, D.; Taschereau, P.; Lee, T. D.; Jurgens, T. *J. Ethnopharmacol.* **2006**, *106*, 360–363. DOI: 10.1016/j.jep.2006.01.018
38. Basu, A.; Sarkar, A.; Maulik, U.; Basak, P. *Indian J. Biochem. Biophys.* **2019**, *56*, 20. DOI: http://nopr.niscair.res.in/handle/123456789/45817
39. Bhal, S. K. *Advanced Chemistry Development*, Toronto, ON, Canada, **2007**, 1-4.
40. Jorgensen, W. L.; Duffy, E. M. *Bioor. Med. Chem. Lett.* **2000**, *10*, 1155-1158. DOI: 10.1016/s0960-894x(00)00172-4